Available online at www.sciencedirect.com
ScienceDirect
Developmental Biology 304 (2007) 467–478
DEVELOPMENTAL BIOLOGY
www.elsevier.com/locate/ydbio

Gastrulation of *Gastrotheca riobambae* in comparison with other frogs

Iván M. Moya, Ingrid Alarcón, Eugenia M. del Pino *

Pontificia Universidad Católica del Ecuador, Escuela de Ciencias Biológicas, Apartado 17-01-2184, Avenida 12 de Octubre y Robles, Quito, Ecuador

Received for publication 31 July 2006; revised 7 December 2006; accepted 15 December 2006
Available online 21 December 2006

Abstract

Blastopore formation, the embryonic disk, archenteron and notochord elongation, and Brachyury expression in the marsupial frog *Gastrotheca riobambae* was compared with embryos of *Xenopus laevis* and of the dendrobatids *Colostethus machalilla* and *Epipedobates anthonyi*. In contrast with *X. laevis* embryos, the blastopore closes before elongation of the archenteron and notochord in the embryos of *G. riobambae* and of the dendrobatid frogs. Moreover, the circumblastoporal collar (CBC) thickens due to the accumulation of involuted cells. An embryonic disk, however, is formed only in the *G. riobambae* gastrula. We differentiate three gastrulation patterns according to the speed of development: In *X. laevis*, elongation of the archenteron and notochord begin in the early to mid gastrula, whereas in the dendrobatids *C. machalilla* and *E. anthonyi* the archenteron elongates at mid gastrula and the notochord elongates after gastrulation. In *G. riobambae*, only involution takes place during gastrulation. Archenteron and notochord elongation occur in the post gastrula. In the non-aquatic reproducing frogs, the margin of the archenteron expands anisotropically, resulting in an apparent displacement of the CBC from a medial to a posterior location, resembling the displacement of Hensen's node in the chick and mouse. The differences detected indicate that amphibian gastrulation is modular.

Keywords: Brachyury; Archenteron; Circumblastoporal collar; Notochord; *Colostethus machalilla*; *Epipedobates tricolor*; *Epipedobates anthonyi*; *Gastrotheca riobambae*

Introduction

The morphological and molecular understanding of gastrulation that derives from the study of development in *Xenopus laevis* provides the basis for the analysis of development in other frogs. In *X. laevis*, dorsal convergence and extension (CE) and blastopore closure are controlled by the planar cell polarity (PCP) pathway, and require a signal mediated by *Dishevelled* (*Xdsh*), whereas mesendoderm internalization and archenteron formation proceeds normally in *Xdsh*-deficient embryos (Wallingford et al., 2002; Ewald et al., 2004). The relative autonomy of gastrulation movements is thought to be a general amphibian feature that may have allowed the evolution of the various modes of frog gastrulation (Ewald et al., 2004). Accordingly, the different frog gastrulation modes may result from changes in the functioning of the PCP pathway.

We studied the gastrulation pattern of the marsupial frog *Gastrotheca riobambae*, previously considered Hylidae, and now Leptodactylidae (Faivovich et al., 2005), and two closely related dendrobatid frogs *Colostethus machalilla* and *Epipedobates anthonyi* (Coloma, 1995; Del Pino et al., 2004; Graham et al., 2004; Santos et al., 2003) in comparison with *X. laevis*. We initiated the study of development in dendrobatids to provide comparative models of frog development (Del Pino et al., 2004). Dendrobatid frogs have several useful features, as they are small, can be obtained commercially in pet shops world wide, reproduce in captivity, and therefore are appropriate for developmental studies.

There are important differences in the development of these non-aquatic reproducing frogs and *X. laevis*. Embryos of *X. laevis* require about 14 h from fertilization to the blastopore slit stage (Nieuwkoop and Faber, 1994). In contrast from fertilization to the completion of gastrulation, the embryos of *C. machalilla* require 4 days and the embryos of *G. riobambae* take 14 days (Del Pino, 1996; Del Pino et al., 2004). Additionally egg size varies among these frogs. The 1.3 mm in diameter eggs of *X. laevis* are the smallest; the eggs of the dendrobatid frogs *C. machalilla* and *E. anthonyi* measure 1.6 mm and 2 mm in diameter, respectively; whereas the eggs of *G. riobambae* are

* Corresponding author. Fax: +593 2 299 1687.
E-mail address: edelpino@puce.edu.ec (E.M. del Pino).

0012-1606/$ - see front matter © 2006 Elsevier Inc. All rights reserved.
doi:10.1016/j.ydbio.2006.12.036

Table 1
Standardized stages of *G. riobambae* gastrulation in comparison with *X. laevis*

X. laevis stage [a]	*G. riobambae* stage [b]	Characteristics of the *G. riobambae* embryos
10	7	Day 7: The early gastrula (Figs. 1A, A′ and 2A, B, D–F). The onset of gastrulation is signaled by the invasion of the transparent and one-cell-thick blastocoel roof by the leading edge of the yolky mesoendoderm (not shown, diagramed in Figs. 1A, A′). Mesendoderm invasion is more pronounced on one side, which may correspond to the dorsal side (left side on Figs. 1A, A′). In the lower region of the marginal zone, the blastoporal-rim, which consists of tiers of circumferentially elongated cells, surrounds the future yolk plug (Figs. 2A, B). In slightly more advanced embryos, bottle cells with small apices were detected in several regions around the circumference of the blastoporal-rim. In other embryos, bottle cells with small apices were found predominantly on one side of the blastoporal-rim (Figs. 2D, E). This area may be the dorsal region. In the vegetal hemisphere, vegetal contraction occurs, and the vegetal cells acquire an elongated shape with small surface apices (Figs. 2D, F). Bra-positive nuclei occur in surface cells around the future yolk plug (not shown; the pattern is similar to *E. anthonyi* stage 12; Fig. 6A). The Brachyury expression of this and other stages is according to Del Pino (1996). Among eight sibling embryos, five had a uniform blastoporal-rim. On one side of the blastoporal-rim of the three remaining embryos there was a field, or a row of bottle cells with small apices.
10.5	7.5	Day 8: The blastoporal groove (Fig. 2C). The shallow blastoporal groove is formed on the likely dorsal side. In some embryos, however, the blastoporal groove is formed simultaneously in more than one region of the blastoporal-rim. Bra is expressed in surface cells around the future yolk plug, as described for stage 10 embryos (Del Pino, 1996). Among 22 sibling embryos the presumed dorsal blastopore lip was detected in 4 embryos (stages 10.5–11, as in Fig. 2C); 6 embryos had round blastopores (stage 12; Figs. 1B, B′ and 3A); and the blastopore was closed in the remaining 12 embryos (stage 12.75; Fig. 3B).
11	7.75	Day 8: The horseshoe-shaped blastopore (Fig. 4A). The shallow dorsal blastoporal groove (Fig. 4A) has advanced laterally. Bra is expressed in surface cells around the blastopore lip.
12	8.0	Day 8: The circular blastopore (Figs. 1B, B′ and 3A). The blastoporal groove continues to be shallow, and it is slightly more pronounced on the presumed dorsal side (to the left in Fig. 1B′). The blastopore is often located in the vegetal region. In some embryos, however, it forms closer to the equator. The yolk plug consists of elongated cells (not shown, comparable to the yolk plug of more advanced embryos; Figs. 4B, D). Bra-positive nuclei occur in surface cells around the blastopore lip (indicated by stippling in Fig. 1B).
12.5	8.5	Day 8: The late gastrula (Figs. 1C, C′ and 4B–D). The blastopore and yolk plug are smaller than in the previous stage. The blastopore lip and the small archenteron are slightly asymmetric towards the likely dorsal side (to the top in Figs. 4B, C). The blastopore lip thickens due to the accumulation of the involuted cells (Fig. 4C). The yolk plug contains bottle-shaped cells (Figs. 4B, D). The blastocoel is large and is covered by a thin roof (Fig. 4B). The surface Bra signal disappears as the blastopore closes.
12.75	8.75	Days 8–11: Blastopore closure and formation of the embryonic disk (Figs. 1D, D′, 3B, C and 4E). In embryos stained for cell borders, the embryonic disk is an area of small cells around the blastopore (Fig. 3B), and in living embryos, the embryonic disk is an area that bulges out on the surface (Fig. 3C). At this stage, the embryonic disk and the thick CBC are equivalent (Fig. 4E). The archenteron is small (Fig. 4E). Once the blastopore closes, the external appearance of the embryos remains unchanged for about 2 days. The surface Bra signal disappears as the blastopore closes.
13	9	Days 11–13: Onset of elongation of the embryonic disk (Figs. 1E, E′, 3D, 4F–6E and 6E). The thick embryonic disk contains the small cells that involuted at the blastopore lip (Fig. 4F), and contains Brachet's cleft (Figs. 4G, G′). The embryonic disk and archenteron are enlarged (Fig. 3D; compare the archenteron in Figs. 4F, H), and the embryo begins an upward rotation. The archenteron floor originally consists of elongated cells with small apices (Fig. 4F), which were previously observed in the yolk plug (Figs. 4B, D). The large CBC becomes displaced in a posterior direction, due to the anisotropic enlargement of the archenteron (Fig. 4H). A new and strong Bra signal is detected in deep cells of the embryonic disk around the closed blastopore. This signal is elongated and indicates the beginning of notochord formation and, consequently the onset of dorsal CE (Fig. 6E). The tip of this signal, opposite the blastopore, signals the anterior region, indicated by an arrow in Fig. 1E.
14	10	Days 13–14: The post gastrula (Figs. 1F, F′, 4I and 6F). Archenteron elongation and dorsal CE occur simultaneously, evidenced by Bra expression in the notochord. Rotation of the embryo is completed and the embryonic disk faces upward (Fig. 4I). With the enlargement of the archenteron, the embryonic disk becomes thinner and somewhat translucent. The thickness of the embryonic disk changes from 10 to 15 cells when the disk is small to 4 cells when the archenteron elongates (Elinson and del Pino, 1985). A strong Bra signal occurs in deep cells and it is restricted to the notochord, tail bud, and surrounding area (Fig. 6F).

[a] Stages of *X. laevis* are according to Nieuwkoop and Faber (1994).
[b] Stages of *G. riobambae* are according to Del Pino (1996).

the largest, with a diameter of 3 mm (Nieuwkoop and Faber, 1994; Del Pino and Elinson, 2003; Del Pino et al., 2004). Moreover, the schedule of gastrulation events varies among these frogs. Elongation and inflation of the archenteron and the elongation of the notochord occur during gastrulation in *X. laevis*, whereas in *C. machalilla* embryos, the archenteron elongates and inflates during gastrulation, and the notochord elongates after blastopore closure. In contrast, all of these processes occur after blastopore closure in *G. riobambae* (Benítez and del Pino, 2002; Del Pino, 1996, 2004; Ewald et al., 2004; Gont et al., 1993). Furthermore, the embryos of *G. riobambae* develop an embryonic disk, a feature that was not detected in other frog embryos (Del Pino and Elinson, 1983; Del Pino, 1996). In this work we re-analyzed gastrulation in *G. riobambae* and studied the elongation and inflation of the archenteron, the circumblastoporal collar (CBC), and the elongation of the notochord in comparison with the other non-aquatic reproducing frogs and *X. laevis*. The CBC is the remnant of the blastopore lip once the blastopore closes (Hausen and Riebesell, 1991). This study provides a basis for comparative studies into the molecular and cellular basis of the variation in the mechanisms of gastrulation.

Materials and methods

Maintenance of frogs and embryos and staging

The procedures for the maintenance of adults and the handling of embryos of the marsupial frog *G. riobambae* and of the dendrobatid frogs *C. machalilla*, and *E. anthonyi* were previously described (Del Pino et al., 2004; Elinson et al., 1990). Embryos of these frogs were produced by natural mating in captivity. Adult *G. riobambae* were purchased from Hyla, Quito, Ecuador, or were collected from Quisapincha, Province of Tungurahua, Ecuador. Adults of *C. machalilla* were collected from three localities, Rio Coaque, Pedernales and Machalilla, Province of Manabí, Ecuador. *E. anthonyi* (Graham et al., 2004), which is also known by its previous names *Epipedobates tricolor* and *Phyllobates tricolor*, was collected from El Progreso, Province of El Oro, and Zarayunga, Province of Azuay, Ecuador. The authorization 016-IC-FAU-DNBAP-MA from the Ministry of the Environment, Ecuador allowed the collection of frogs.

The gastrulation stages of *G. riobambae* are according to our previous work, and to facilitate comparison we provide the equivalence with the *X. laevis* developmental stages (Nieuwkoop and Faber, 1994; Del Pino, 1996). Gastrulae of all frogs were staged according to the *X. laevis* normal table of stages (Nieuwkoop and Faber, 1994; Del Pino et al., 2004).

Silver staining of cell boundaries

The staining of the cell surface was done as described for the medaka (Kageyama, 1980). After mechanical removal of the outer layers of egg jelly, the embryos were fixed in Stockerd's solution for up to 10 s. The embryos were rinsed twice with distilled H_2O, followed by incubation in 0.01% silver nitrate for 20–30 s. The embryos were again rinsed with distilled H_2O and were exposed to strong sunlight, immersed in water. Embryos were photographed immediately. Stockerd's solution contains 5 ml of 37% formaldehyde, 6 ml glycerol, 4 ml glacial acetic acid, and 85 ml distilled H_2O (Kageyama, 1980). Stockerd's solution was prepared shortly before use. The silver stained embryos were stored at −20 °C in Dent's solution (Dent et al., 1989).

Embryo fixation and sectioning

The embryos were fixed overnight at room temperature in Smith's solution (Smith, 1912). Smith's solutions was prepared before use by mixing two solutions in equal proportions (solution A: 1% $K_2Cr_2O_7$ in distilled H_2O; solution B: 200 ml 37% formaldehyde, 50 ml acetic acid and 750 ml distilled H_2O). After fixation, the embryos were washed three times with distilled H_2O and stored in 4% formaldehyde in Phosphate Buffered Saline solution (PBS; 137 mM NaCl, 3 mM KCl, 1.5 mM KH_2PO_4, 7 mM Na_2HPO_4; pH 7.4) at 4°C until processing.

Fixed embryos were bisected in glycerol or were cut after embedding in 6% agarose in PBS. The bisected embryos were incubated in 7.5% gelatin in PBS at 45 °C for 4 h. The blastocoel acquired its normal shape by the ingression of gelatin into this cavity. Moreover, gelatin filled in the spaces between the large yolky blastomeres, and facilitated the handling and cutting of sections. The embryos were embedded in 6% agarose in PBS, and sections of 50–100 μm were produced with a Vibratome 1000 (Technical Products International, Inc., St. Louis, MO, USA) as previously described (Del Pino, 1996). To detect cell nuclei, some sections were stained for 1–20 min with Hoechst 33258 (Sigma-Aldrich, St. Louis, MO, USA), extensively rinsed in PBS, mounted in glycerol, and examined with fluorescent optics.

Whole mount immunostaining

For whole mount immunostaining with an anti-Bra antibody (Kispert and Herrmann, 1994), the embryos were fixed in MEMFA buffer (Harland, 1991). The secondary antibody was sheep anti-rabbit IgG conjugated to alkaline phosphatase (Boehringer Mannheim GmbH, Mannheim, Germany). Immunostaining was done as previously described (Benítez and del Pino, 2002; Kuratani and Horigome, 2000). Embryos were analyzed and photographed with a Stemi SV 6 and with an Axiophot (Carl Zeiss, Oberkochen, Germany).

Results

Standardized stages of gastrulation in G. riobambae

This study is restricted to the analysis of blastopore formation, the embryonic disk, archenteron and notochord elongation, and Brachyury expression in embryos of *G. riobambae* in comparison with other non-aquatic reproducing frogs and *X. laevis* embryos, as described in the following sections (Figs. 2–6). To facilitate the comparison of gastrulation, we provide a description of the *G. riobambae* stages of

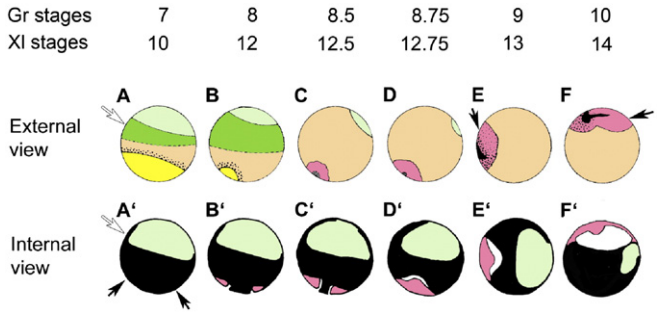

Fig. 1. Standardized stages of gastrulation in *G. riobambae*, modified from Del Pino (1996). The description of each stage is given in Table 1. (A–F) External morphology. The blastocoel floor is indicated by a broken line in panels A, B. The dorso-anterior side is indicated by an arrow in panels E, F. Bra expression is indicated by fine stippling to signal the expression in surface cells (A, B), and by tick stippling and solid black regions to indicate the deep Bra signal (E, F). In stages 12.5–12.75, no Bra-signal was detected (C, D). (A′–F′) Internal morphology. The white arrow in panels A, A′ points to the leading edge of the mesendoderm. Vegetal contraction occurs in the vegetal area between the black arrows in panel A′. Colors: light green is the blastocoel; dark green is the translucent blastocoel invaded by the mesendoderm; beige is the opaque yolky region; yellow is the yolk plug; pink is the involuted cells and the embryonic disk; white is the archenteron; black indicates other regions of the embryo in panels A′–F′. Colors do not represent the germ layers.

gastrulation and their equivalence with *X. laevis* (Table 1; Fig. 1; *G. riobambae* embryos are shown in Figs. 2A–F, 3A–D, 4A–I, and 6E–F) (Del Pino and Elinson, 1983; Elinson and del Pino, 1985; Nieuwkoop and Faber, 1994; Del Pino, 1996). Dorsal–ventral axis in the gastrula of all frogs is described according to the traditional model for amphibian axial patterning, reviewed in (Wolpert et al., 2007). An alternative fate map reassigns the dorso-ventral axis of the traditional model to the rostro-caudal axis, reviewed in (Lane and Sheets, 2006).

Comparison of blastopore formation

Before formation of the blastopore, a uniform blastoporal-rim was observed around the future yolk plug of *G. riobambae* embryos. On the surface, the blastoporal-rim consisted of several tiers of circumferentially elongated cells (Figs. 2A, B). In sagittal view these cells could not be identified, as they resembled other cells of this region (not shown). In somewhat more advanced embryos, a field or a row of bottle cells with small apices was found in the presumed dorsal side of the previously symmetric blastoporal-rim (Figs. 2D, E). Scattered bottle cells were also found in the lateral and ventral sides of the blastoporal-rim (not shown). Thereafter, a small blastopore groove and the presumed dorsal blastopore lip developed (Fig. 2C).

In embryos of *C. machalilla*, in contrast, the blastoporal-rim developed gradually. At first, several tiers of circumferentially elongated cells were detected only in the dorsal

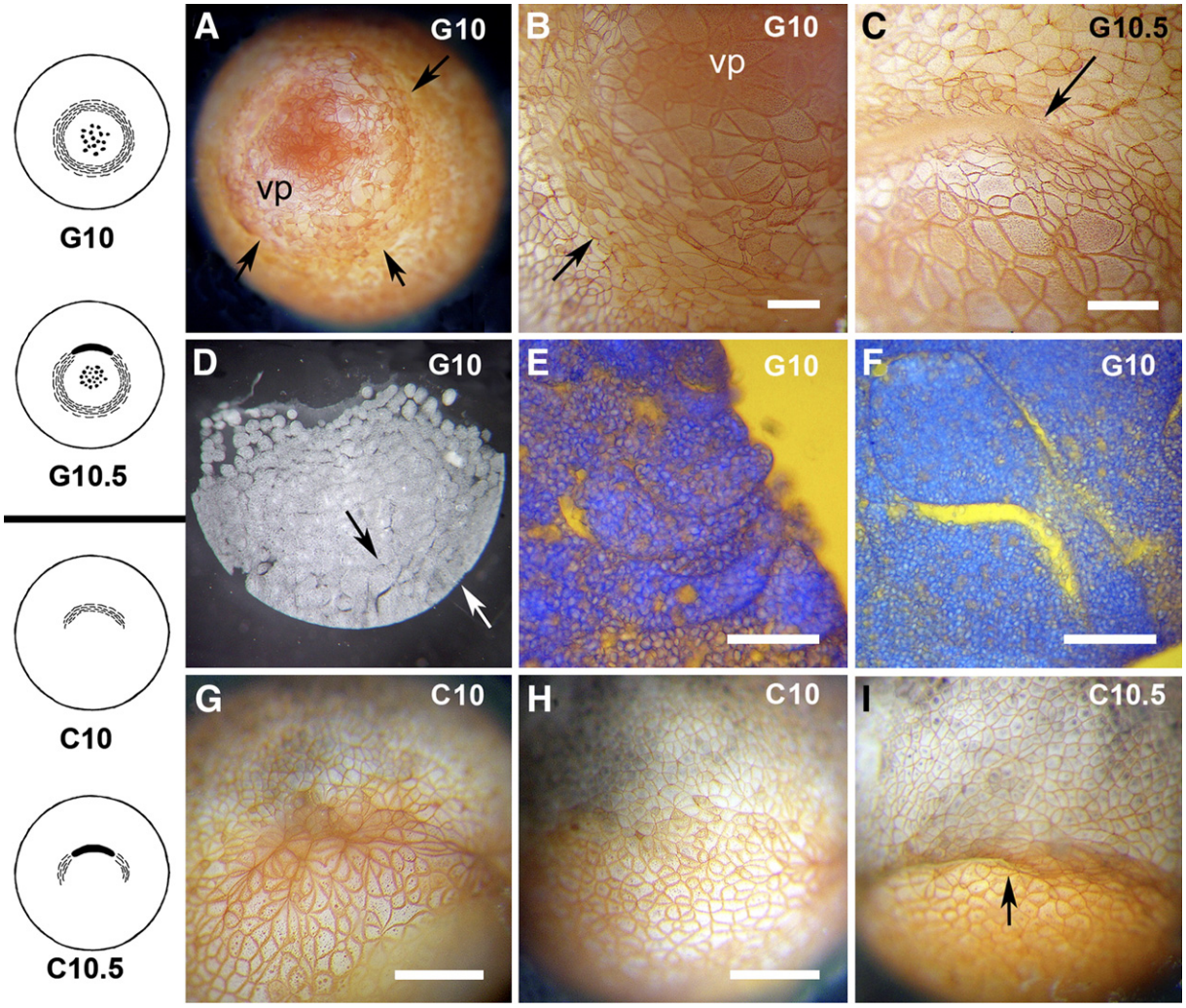

Fig. 2. Blastopore lip formation in *G. riobambae* and *C. machalilla*. Embryos are stained for cell borders in panels A–C, G–I. (A–F) Embryos of *G. riobambae*. (A) Vegetal view of an early gastrula. Arrows indicate the blastoporal-rim. (B) Higher magnification of the tiers of circumferentially elongated cells in the blastoporal-rim. (C) Blastoporal groove. The arrow signals the lateral limit of the groove. (D) Sagittal section of an early gastrula. To the right, there is a field of bottle cells (white arrow). Cells in the vegetal region are bottle-shaped (black arrow). (E) Higher magnification of the field of bottle cells (white arrow in panel D). (F) Higher magnification of a vegetal bottle-shaped cell (black arrow in panel D). (G–I) Embryos of *C. machalilla*. (G) A rim of circumferentially elongated cells occurs in the region of the future dorsal blastopore lip. (H) Ventral view from the embryo in panel G. (I) The dorsal blastopore lip, an arrow indicates its lateral limit. To facilitate the comparison, in this and the following figures the number in the upper right-hand corner gives the standardized stage, and the letter indicates the species: G, *Gastrotheca riobambae*; C, *Colostethus machalilla*; E, *Epipedobates anthonyi*; and X, *Xenopus laevis.* Drawings of the vegetal features are given on the left: Tiers of circumferentially elongated cells of the blastoporal-rim are represented by small lines. Vegetal cells with contracted apices are indicated by black dots. The blastopore groove is indicated by a thick line. Abbreviations: vp, vegetal pole. Bars represent: 100 μm in panels E, F; 300 μm in panel C; 400 μm in panels G, H; 500 μm in B.

region (Figs. 2G, H). Later, after formation of the blastopore groove in the dorsal side, tiers of circumferentially elongated cells were observed laterally (Fig. 2I), and then ventrally. In *X. laevis* embryos, the formation of six to eight tiers of circumferentially elongated cells at the vegetal end of the involuting marginal zone precedes the appearance of typical bottle cells with small surface apices, and the formation of the blastopore groove (Hardin and Keller, 1988). A circular blastoporal-rim as described for *G. riobambae* was not detected in *C. machalilla* (compare Figs. 2A, B with Figs. 2G, H), nor in *X. laevis* (Hardin and Keller, 1988). Once the blastopore lip was formed, bottle cells were found at the anterior tip of the archenteron in *G. riobambae* (Elinson and del Pino, 1985) and *C. machalilla* embryos (not shown), as in embryos of *X. laevis*.

Involution and archenteron formation advanced more rapidly in the presumed dorsal region of the *G. riobambae* gastrula, although the blastopore lip remained shallow (Figs. 2C, 3A, and 4A–C). In contrast, the embryos of *C. machalilla* and *E. anthonyi* developed a well-defined subequatorial dorsal blastopore lip, and the external morphology of the dorsal lip and of the blastopore resembled the gastrula of *X. laevis* and other frogs (Figs. 2G, I and 3E–F). The external morphology of the *E. anthonyi* early gastrula is similar with that of *C. machalilla* (not shown).

The early gastrula of *G. riobambae* undergoes contraction of the vegetal surface by about 50% (Elinson and del Pino, 1985). Vegetal contraction is a common morphogenetic movement observed during gastrulation of urodeles and anurans, including *X. laevis* (Ballard, 1955; Keller, 1978; Elinson and del Pino, 1985). In *G. riobambae* embryos, this movement is associated with the formation of bottle-like cells in the vegetal pole region (Figs. 2D, F and 4A), and with the appearance of a pit in the central region of the yolk plug (not shown). It is unknown whether these bottle-shaped cells actually leave the surface. Once the blastopore was formed, the yolk plug contained bottle-like cells with small surface apices, as seen in sagittal view

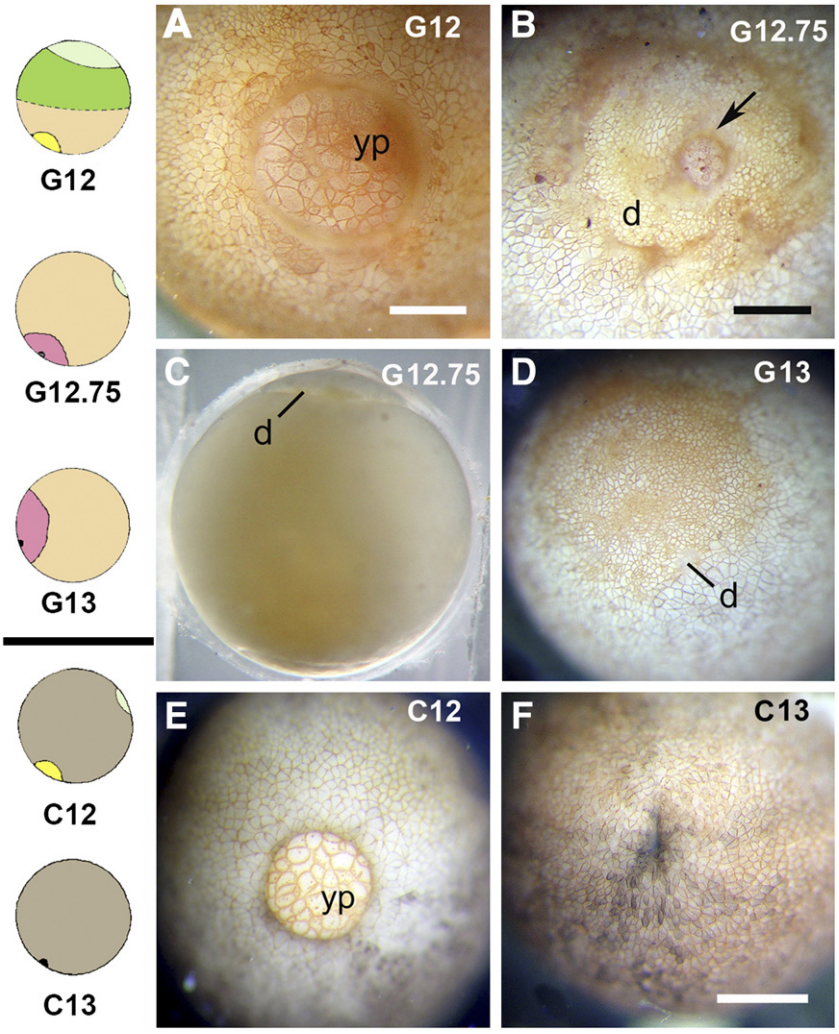

Fig. 3. Surface view of blastopore closure in *G. riobambae* and *C. machalilla*. All embryos are stained for cell borders, except for the embryo in panel C. (A–D) Embryos of *G. riobambae*. (A) Circular blastopore. (B) Blastopore closure and the embryonic disk. The arrow signals the yolk plug. (C) The embryonic disk of a living embryo in lateral view. (D) The embryonic disk in an embryo stained for the cell borders. (E–F) Embryos of *C. machalilla*. (E) Embryo with a circular blastopore. (F) Embryo with a closed blastopore. The drawings on the left give the features of each stage. Drawings on the left are as in Fig. 1, except that the Bra signal has been deleted. Abbreviations: d, disk; yp, yolk plug. Bars represent 400 μm in panel F; 500 μm in panels A, B.

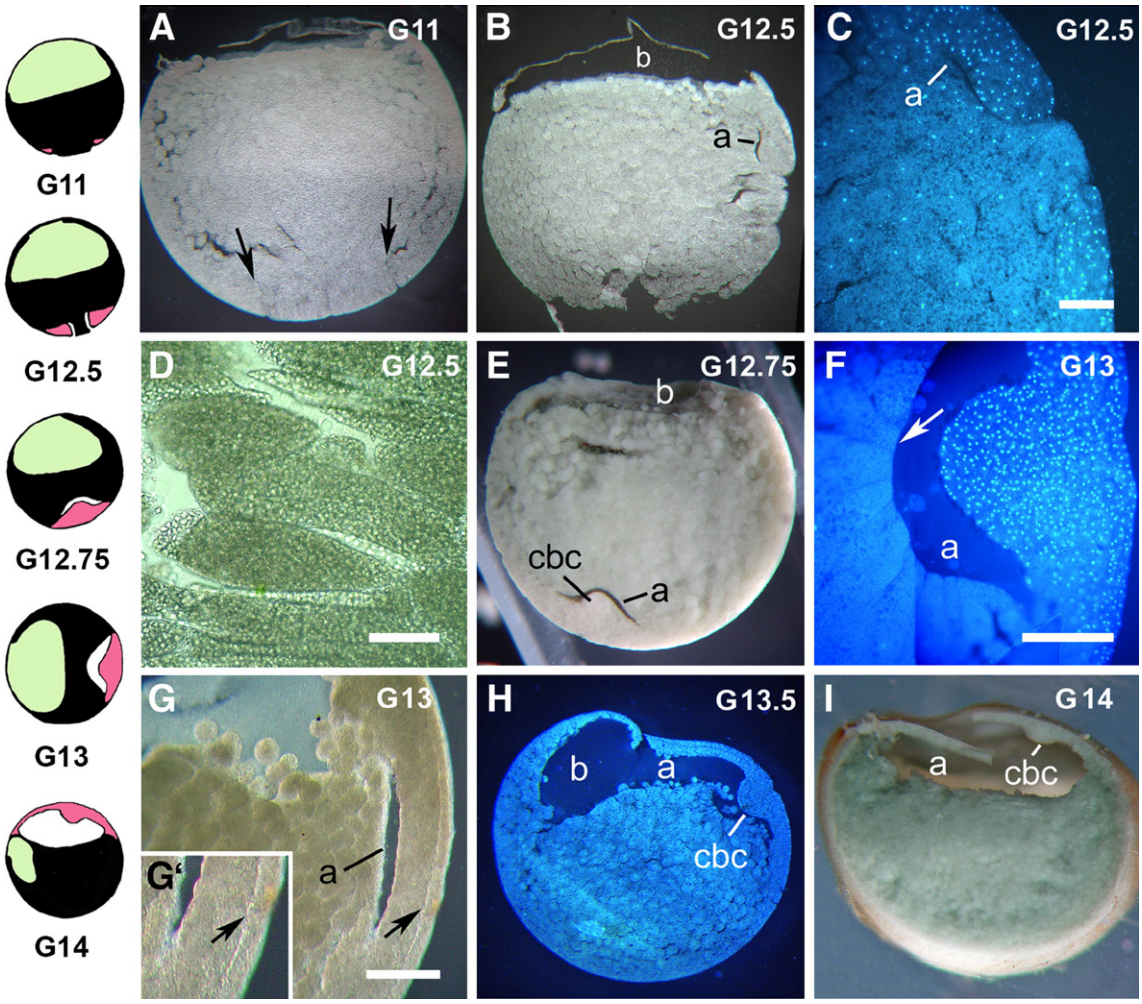

Fig. 4. Internal morphology of the *G. riobambae* gastrula. (A) Sagittal section of a stage 11 embryo. The blastopore lip is indicated by arrows. (B) Sagittal section of an embryo with a blastopore, located near the equator. (C) Sagittal section of an embryo (as in panel B), stained for cell nuclei. (D) Higher magnification of the yolk plug. (E) Sagittal bisection of an embryo with a closed blastopore. (F) Sagittal section stained for cell nuclei from an embryo at the onset of archenteron elongation. The archenteron floor is indicated by an arrow. (G) Para-sagittal section of an embryo with a closed blastopore. The CBC contains Brachet's cleft (arrow). (G′) Higher magnification of Brachet's cleft (arrow). (H) Sagittal section of a post gastrula. The limit between the blastocoel and the archenteron is fractured. (I) Bisection of a post gastrula. The drawings on the left are as in Fig. 1. Abbreviations: a, archenteron; b, blastocoel; cbc, circumblastoporal collar. Bars represent 300 μm in panel C; 50 μm in panel D; 100 μm in panel F; 400 μm in panel G.

(Figs. 4B, D). Moreover, after blastopore closure, the floor of the small archenteron, which derives from the yolk plug, still contained cells with small surface apices and bottle-like appearance (Fig. 4F). Bottle-shaped cells in the archenteron floor were no longer observed after archenteron elongation at stages 13.5–14 (not shown). It seems that the formation of bottle-shaped cells contributes to internalize the large amount of archenteron floor inside the embryo.

The embryonic disk of G. riobambae in comparison with other frogs

The unique feature of the *G. riobambae* gastrula is the formation of an embryonic disk, around the closing blastopore (Del Pino and Elinson, 1983). The embryonic disk protruded on the embryonic surface of *G. riobambae* embryos (Figs. 3B, C). After silver staining of superficial cell-boundaries, the embryonic disk was detected as an area of small cells around the small yolk plug (Figs. 3B, D). In contrast, an embryonic disk was not detected on the surface of the *X. laevis*, *Eleutherodactylus coqui*, and *C. machalilla* gastrulae (Figs. 3E, F) (Del Pino and Elinson, 1983). Formation of the embryonic disk in *G. riobambae* embryos was associated with delayed elongation of the archenteron and the accumulation of involuted cells in the blastopore lip (Fig. 4C). These features resulted in the formation of a conspicuous CBC in the late gastrula (Fig. 4E).

The recently formed archenteron of *G. riobambae* embryos was at first very small, and it enlarged only after blastopore closure (Figs. 4E–I). From the beginning, the archenteron was slightly larger on the presumed dorsal side (Figs. 4B, C). The dorso-anterior asymmetry of the archenteron became more pronounced 2 days after blastopore closure when the archenteron simultaneously elongated and became inflated (Figs. 4H, I). Elongation and inflation of the archenteron occurred in coincidence with the elongation of the embryonic disk and the

notochord, as detected by Bra expression in the notochord (Figs. 4I and 6E–F).

As in *G. riobambae*, the archenteron remained small during gastrulation in *C. machalilla* and *E. anthonyi*, and the involuted cells remained in the blastopore lip (Figs. 5A–D, G–H). Moreover, the blastopore lip formed a conspicuous CBC (Figs. 5E, F, I), which apparently contained the majority of the involuted cells, as suggested by the density of cell-nuclei in this region, as shown for *C. machalilla* (Figs. 5E, F). In contrast with *G. riobambae*, elongation and inflation of the archenteron in these dendrobatid frogs began in the late gastrula (Figs. 5B–D, H). Archenteron elongation occurred in a dorso-anterior direction,

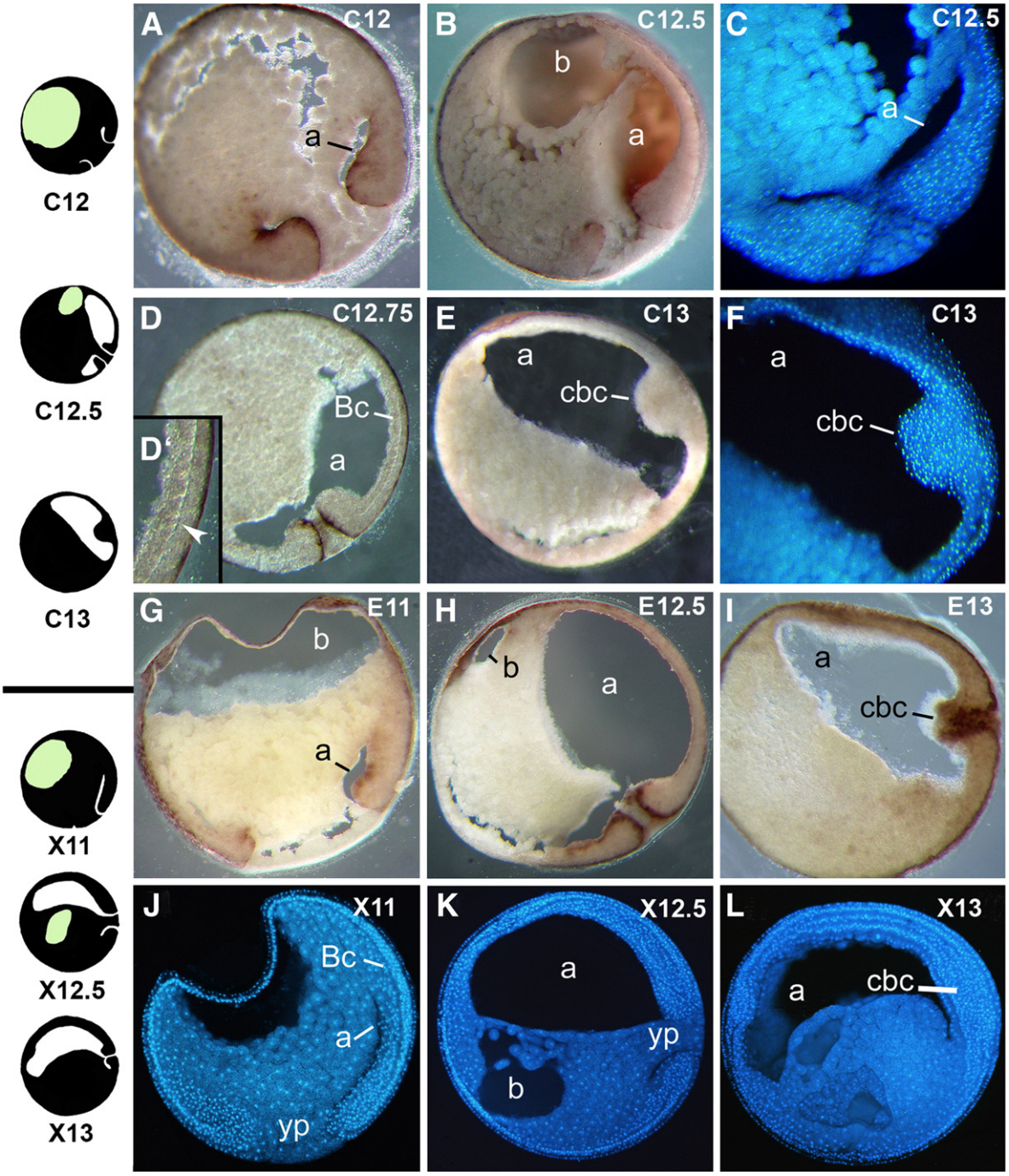

Fig. 5. Internal view of blastopore closure in *C. machalilla*, *E. anthonyi* and *X. laevis*. The dorsal side is to the right in all images. (A–F) Embryos of *C. machalilla.* (A) Sagittal section of a mid gastrula. The archenteron is slightly larger on the dorsal side (a). (B) Sagittal bisection of a late gastrula. (C) Parasagittal section stained for cell nuclei. (D) Sagittal section of a slightly more advanced embryo. (D′) Higher magnification of the cleft of Brachet region (arrow). (E) Sagittal section of an embryo with a closed blastopore. (F). The CBC stained for cell nuclei. (G–I) Embryos of *E. anthonyi*. (G) Late stage 11 embryo. (H) Sagittal section of a late gastrula. (I) Sagittal section from an embryo with a closed blastopore. (J–L) Embryos of *X. laevis* stained for cell nuclei. (J) Sagittal section of stage 11 embryo. (K) Sagittal section of a late gastrula. (L) Para-sagittal section of a post gastrula. The images on the left were rotated from those in Fig. 7. Abbreviations: a, archenteron; b, blastocoel; Bc, cleft of Brachet; cbc, circumblastoporal collar; yp, yolk plug.

and the anisotropic enlargement of the archenteron shifted the CBC in a posterior direction (Figs. 5D–F), as in *G. riobambae* (Figs. 4H–I); this feature resembles the posterior displacement of Hensen's node in the chick embryo as the notochord elongates.

Embryos of *E. anthonyi* elongated and inflated the archenteron somewhat earlier than those of *C. machalilla* (Figs. 5A, G), and its CBC was less pronounced (Figs. 5E, I). The gastrulation pattern of these closely related species is similar, in spite of the slight difference in egg size. The notable aspect of dendrobatid frog gastrulation is the formation of a conspicuous CBC, which morphologically resembles the CBC of *G. riobambae* gastrulae, although the dendrobatid frog embryos do not form an embryonic disk.

The gastrula of *X. laevis* differed from the previously analyzed frogs, as archenteron elongation, its inflation and the elongation of the notochord occurred during gastrulation, and the involuted cells moved away from blastopore lip due to the movements of CE on the dorsal lip (Figs. 5J, K and 6H). The resulting CBC was small and had a posterior location (Fig. 5L). In embryos of *X. laevis* elongation of the archenteron was separated from its inflation (Figs. 5J, K), as previously demonstrated (Ewald et al., 2004), and in contrast with the other frogs analyzed in this work. Epiboly and dorsal CE are thought to drive different aspects of archenteron elongation, as this process was independent of *Xdsh*-signal during the second half of *X. laevis* gastrulation (Ewald et al., 2004). In dendrobatid frog embryos, forces other than CE may drive the initial elongation of the archenteron, as its elongation starts before elongation of the notochord.

Brachet's cleft was detected in the blastopore lip *G. riobambae*, *C. machalilla*, and *X. laevis* embryos, and in the embryonic disk of *G. riobambae* embryos (Figs. 4G, G′ and 5D, D′, J). Brachet's cleft is an indication of involution at the blastopore lip in *X. laevis* (Wacker et al., 2000), and possibly also in the other frog embryos analyzed. Direct evidence of involution was the internalization of vital dye marks that were placed around the blastopore of *G. riobambae* and *C. machalilla* embryos (work in progress) (Del Pino and Elinson, 1983; Elinson and del Pino, 1985).

Comparison of Brachyury expression and notochord elongation

We compared Bra expression in the embryos of *E. anthonyi* with *X. laevis*, *G. riobambae* and *C. machalilla* (Smith et al., 1991, Del Pino, 1996; Benítez and del Pino, 2002). In the *E. anthonyi* early to mid gastrula we detected few superficial Bra-positive nuclei around the blastopore (Fig. 6A). In the late gastrula, few superficial Bra-positive nuclei remained, and a strong Bra-signal was detected in a deep ring of cells around the blastopore (Fig. 6B). The notochord of *E. anthonyi* embryos was not detected during gastrulation (Figs. 6A–C), and it elongated after closure of the blastopore (Fig. 6D). This pattern is similar with the Bra expression pattern of *C. machalilla* embryos (Benítez and del Pino, 2002). As in *E. anthonyi* (Fig. 6A), the superficial Bra-positive signal around the blastopore disappeared during blastopore closure in *G. riobambae* embryos (not shown). After blastopore closure at the onset of archenteron elongation, a deep Bra-signal was detected around the blastopore, and its apex signaled the dorso-anterior region (to the left in Fig. 6E). Thereafter, the notochord developed (Fig. 6F). The pattern of Bra expression at the protein level in embryos of *X. laevis* is shown in Figs. 6G, H. In the *X. laevis* mid gastrula, we detected a deep ring of Bra-positive nuclei around the blastopore (Fig. 6G). In the late gastrula, Bra-positive nuclei were detected around the still open blastopore and in the notochord (Fig. 6H). Surface Bra-positive nuclei were not detected in the *X. laevis* gastrula. The Bra-protein expression pattern is similar with the mRNA pattern previously reported (Smith et al., 1991; Gont et al., 1993).

Discussion

We recognize three patterns of frog gastrulation according to the speed of development (Fig. 7). These patterns are exemplified by gastrulation in *X. laevis*, the dendrobatids *C. machalilla* and *E. anthonyi*, and the marsupial frog *G. riobambae* (Fig. 7). In the rapidly developing embryos of *X. laevis*, archenteron and notochord elongation occurs simultaneously with involution and closure of the blastopore. In contrast, in the slow developing *G. riobambae* involution occurs during gastrulation, whereas archenteron and notochord elongation occur in the post gastrula, after blastopore closure. The pattern of gastrulation in *C. machalilla* and *E. anthonyi* is intermediate when compared to *X. laevis* and *G. riobambae* such that archenteron elongation occurs in the mid gastrula and notochord elongation in the post gastrula (Fig. 7).

In *X. laevis*, elongation of the archenteron, dorsal CE, and notochord elongation begin in the early to mid gastrula as detected morphologically and by Bra expression (Youn et al., 1980; Gont et al., 1993). Moreover, dorsal CE directs blastopore closure (Keller, 1986; Youn et al., 1980). In the ventral blastopore lip, in contrast, convergence occurs in absence of extension, and the ventral blastopore lip thickens, where presumptive somatic mesoderm is held in reserve for addition to the dorsal axis. This movement, called convergence and thickening (CT), may guide blastopore closure in the ventral side of *X. laevis* embryos (Keller and Shook, 2004).

The pattern of *G. riobambae* gastrulation differs from *X. laevis*. It was proposed that formation of the embryonic disk of *G. riobambae* embryos may result from a delay in dorsal CE (Keller and Shook, 2004). The cells at the blastopore lip may undergo CT, contributing to close the blastopore, and leading to the formation of the embryonic disk. After closure of the blastopore, dorsal CE is thought to guide notochord elongation (Keller and Shook, 2004). This interpretation is in agreement with our observations. The blastoporal-rim of *G. riobambae* embryos may morphologically represent the onset of CT (Fig. 2A). It may be that CT occurs around the blastopore in *G. riobambae*, followed by dorsal CE, whereas in *C. machalilla* and *X. laevis*, the gradual appearance of the blastoporal-rim suggests that CT on the dorsal side may occur first, followed CT

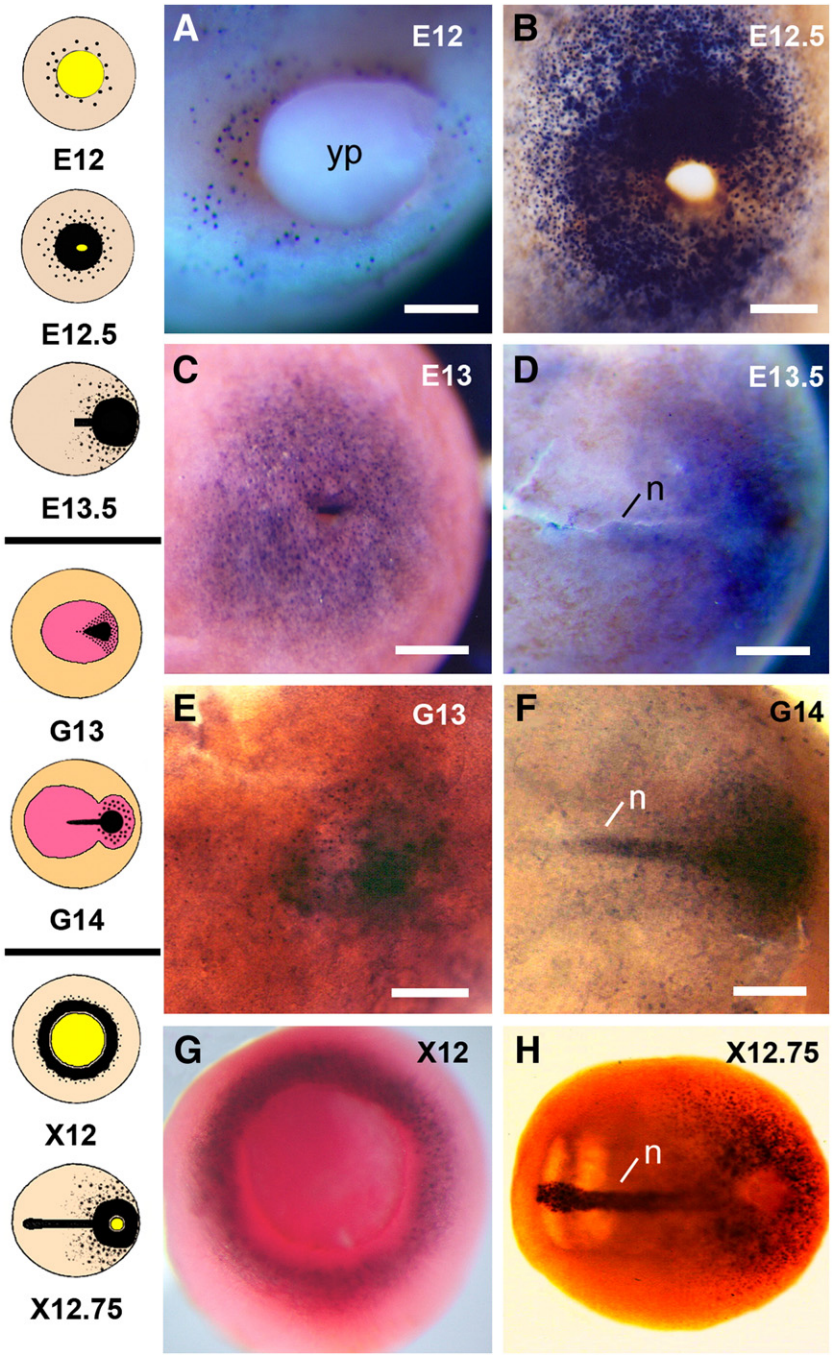

Fig. 6. Brachyury expression in *E. anthonyi*, *G. riobambae* and *X. laevis* embryos. All embryos were immunostained with anti-Bra and were cleared, except for the embryos in panels A, C. (A–D) Embryos of *E. anthonyi*. (A) Surface signal around the blastopore. (B) Deep signal around the open blastopore. (C) Surface and deep signal around the closed blastopore. (D) Deep signal in the notochord and around the closed blastopore. (E–F) Embryos of *G. riobambae*. (E) Deep signal around the closed blastopore. Anterior is to the left. (F) Deep signal in the notochord and around the closed blastopore. (G–H) Embryos of *X. laevis*. (G) Deep signal around the blastopore. (H) Deep signal around the still open blastopore, and in the notochord. The drawings on the left outline the Bra expression pattern. The Bra signal is shown by black dots and black areas, other colors as in Fig. 1. Abbreviations: n, notochord. Bars represent: 200 μm in panels A, B; 400 μm in panels C, F; 300 μm in panels D, E.

on the lateral and ventral sides and by dorsal CE (Figs. 2G–I) (Hardin and Keller, 1988).

In the embryos of *X. laevis*, the anterior region of Brachet's cleft is formed by vegetal rotation, whereas the Brachet's cleft posterior area is formed by the involution at the blastopore lip (Winklbauer and Schüferld, 1999). A similar pattern occurs in the frogs analyzed in this work. In fact in the early gastrula, we detected the anterior region of Brachet's cleft, which was formed by the invasion of the presumed mesendoderm along the blastocoel roof (not shown). This tissue separation suggests that vegetal rotation may also occur in the embryos of these frogs. Moreover, the detection of Brachet's cleft in the blastopore lip, the embryonic disk, and in the CBC of *G. riobambae* and *C. machalilla* embryos suggests that the neuroectoderm and

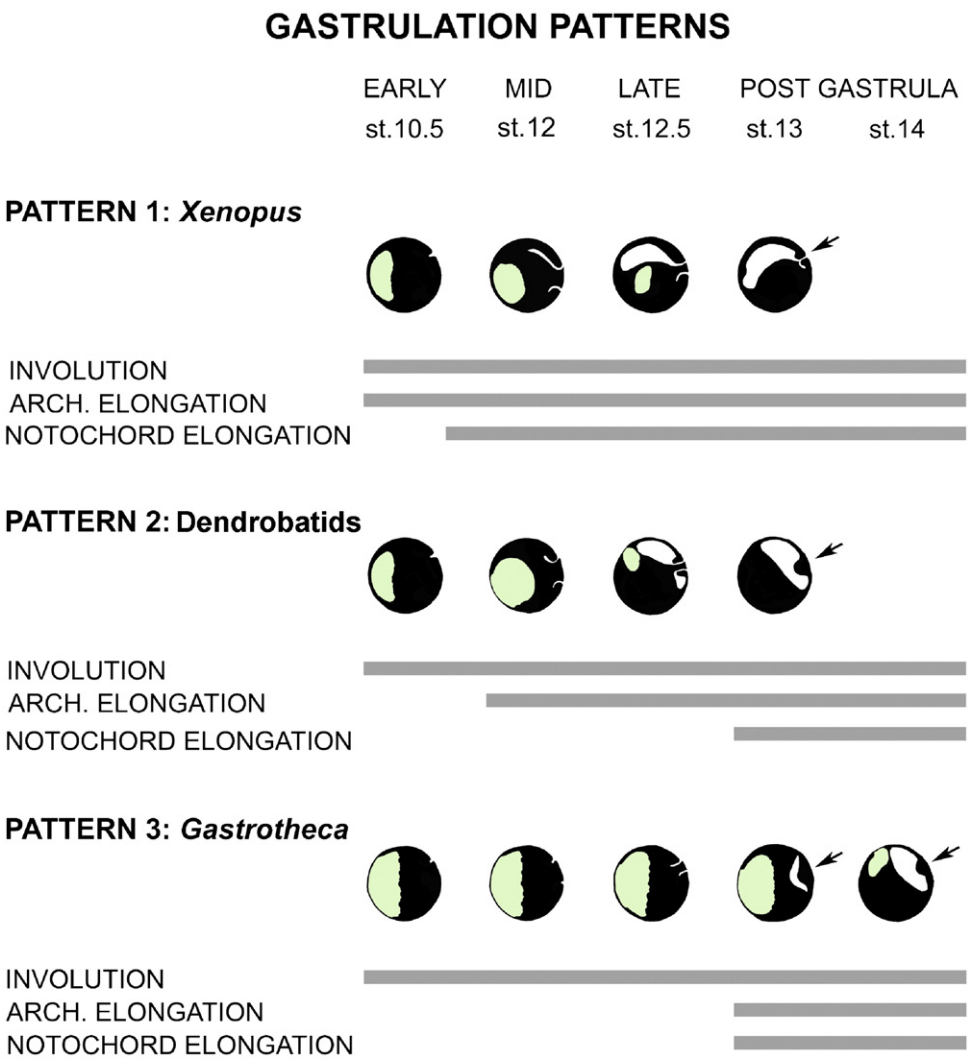

Fig. 7. Gastrulation patterns. Dorsal is oriented toward the top. Involution, archenteron and notochord elongation are indicated by bars. Pattern 1: *Xenopus*. Rapid development (14 h from fertilization to the end of gastrulation). Pattern 2: Dendrobatid frogs. Slow development (4 days from fertilization to the end of gastrulation). Pattern 3: *Gastrotheca.* Very slow development (14 days from fertilization to the end of gastrulation). The arrows indicate the circumblastoporal collar. Colors as in Fig. 1. Gastrulation patterns are discussed in the text.

endomesoderm are already separated in these structures, as in the blastopore lip of *X. laevis* (Wacker et al., 2000). In contrast with *X. laevis*, elongation of the notochord is delayed in the embryos of these non-aquatic reproducing frogs, suggesting that the tissue separation at Brachet's cleft may be independent of dorsal CE.

The simultaneous occurrence of gastrulation and of other dorsal morphogenetic events in the *X. laevis* gastrula probably relate to the complex gene expression pattern of the dorsal blastopore lip. In contrast, the dorsal lip in frogs with slow development may have a less complex pattern of gene expression, due to the retardation of dorsal CE. Unfortunately, the information about gene expression during gastrulation is quite limited for frogs other that *X. laevis* (Del Pino and Elinson, 2003). Only the pattern of Bra expression is known for all of the analyzed frogs. In vertebrates, *Bra* is needed for gastrulation movements, and for the differentiation of the posterior mesoderm and notochord, reviewed in Herrmann and Kispert (1994) and Smith (1999). In *X. laevis* embryos, *Bra* is an early response gene to mesoderm induction. It is expressed in a deep ring of cells located in the equatorial region of the early gastrula, and later around the closing blastopore (Smith et al., 1991). *Brachyury* expression in the notochord begins in the early to mid gastrula and indicates the onset of dorsal CE (Smith et al., 1991; Gont et al., 1993).

The few superficial Bra-positive cells around the blastopore of the early gastrula in *E. anthonyi* (Fig. 6A), *G. riobambae*, and *C. machalilla* lack a counterpart in the embryos of *X. laevis*, but the internal Bra-positive ring detected around the closing blastopore resembles the Bra expression signal of *X. laevis* embryos (Figs. 6B–F) (Smith et al., 1991; Del Pino, 1996; Benítez and del Pino, 2002). Accordingly, in frogs with slow development the mesoderm may become specified later than in *X. laevis*, resulting in a deep Bra signal around the blastopore of the late gastrula (Fig. 6B). In support of this view it is known that interference with *Bra* function inhibits dorsal

CE, and notochord differentiation in *X. laevis* (Conlon and Smith, 1999). Moreover, the PCP pathway that guides dorsal CE may be similarly delayed, as it is known that *XWnt11*, a component of the PCP pathway, is a direct target of *Xbra* (Tada and Smith, 2000). Additionally, in *Ciona intestinalis* specific notochordal genes are also downstream of *CiBra* (Hotta et al., 2000). The differences observed emphasize the need for cell lineage studies in *G. riobambae* and in the dendrobatid frogs to determine the location of the prospective mesoderm. Similarly, the onset of dorsal CE should be determined experimentally in these frogs. Further study will indicate whether the patterning elements that guide CE also occur during CT. It will be important to compare the molecular mechanisms of Brachet's cleft formation in these different frogs, as it is known that tissue separation behavior at Brachet's cleft is controlled by the non-canonical Wnt signaling in *X. laevis* (Winklbauer et al., 2001). Additionally, it will be important to know whether signaling through *Dsh*, which is responsible for dorsal CE and for the closure of the blastopore in *X. laevis* (Ewald et al., 2004), is retarded in the embryos of *G. riobambae.*

The *X. laevis* gastrula has two molecular centers or organizers, the dorsal and the ventral gastrula centers, whose molecular characterization is rapidly advancing (De Robertis, 2006). The relative independence of these gastrula organizers detected for *X. laevis* (Ewald et al., 2004) is interesting in the context of the different morphologies of gastrulation that occur in nature. In fact, ventralized *X. laevis* embryos by either injection of suramin into the blastocoel or by ultraviolet irradiation in the vegetal region (Gerhart et al., 1989; Scharf et al., 1989) resemble the morphological features of the *G. riobambae* gastrula. Similarly, *dsh*-deficient *X. laevis* embryos concentrate the involuted cells in the blastopore lip, do not extend the notochord, and their morphology is also comparable to the gastrulae of *G. riobambae* (Ewald et al., 2004). Our work suggests that amphibian gastrulation is modular and that the gastrulation patterns of different frogs may depend on modified timing of gene expression whose analysis may aid in better understanding gastrula development.

Acknowledgments

We thank B. Herrmann (Max-Planck-Institute for Immunology, Freiburg, Germany) for providing us with anti-Bra. Thanks are expressed to D. Donoso and S. Benítez for help with the immunostaining of *E. anthonyi* embryos, to O. D. Pérez for helpful discussions and scientific assistance, and to L. E. López for his help in obtaining the frogs. We thank I. B. Dawid for the critical reading of the manuscript. We acknowledge the grants from the Foundation for Science and Technology of Ecuador; grant number FUNDACYT-034, and the Pontificia Universidad Católica del Ecuador for its 2003, 2004, 2005 grants.

References

Ballard, W.W., 1955. Cortical ingression during cleavage of amphibian eggs, studied by means of vital dyes. J. Exp. Zool. 129, 77–98.

Benítez, M.-S., del Pino, E.M., 2002. The expression of Brachyury during development of the dendrobatid frog *Colostethus machalilla*. Dev. Dyn. 225, 592–596.

Coloma, L.A., 1995. Ecuadorian frogs of the genus *Colostethus* (Anura: Dendrobatidae). Miscellaneous Publications. Natural History Museum. University of Kansas, Lawrence, 87, 1–74.

Conlon, F.L., Smith, J.C., 1999. Interference with *Brachyury* function inhibits convergent extension, causes apoptosis, and reveals separate requirements in the FGF and activin signaling pathways. Dev. Biol. 213, 85–100.

De Robertis, E.M., 2006. Spemann's organizer and self-regulation in amphibian embryos. Nat. Rev., Mol. Cell Biol. 7, 296–302.

del Pino, E.M., 1996. The expression of Brachyury (T) during gastrulation in the marsupial frog *Gastrotheca riobambae*. Dev. Biol. 177, 64–72.

del Pino, E.M., Elinson, R.P., 1983. Gastrulation produces an embryonic disc, a novel developmental pattern for frogs. Nature 306, 589–591.

del Pino, E.M., Elinson, R.P., 2003. The organizer in amphibians with large eggs: problems and perspectives. In: Grunz, H. (Ed.), The Vertebrate Organizer. Springer, Berlin, pp. 359–374.

del Pino, E.M., Ávila, M.E., Pérez, O.D., Benítez, M.-S., Alarcón, I., Noboa, V., Moya, I.M., 2004. Development of the dendrobatid frog *Colostethus machalilla*. Int. J. Dev. Biol. 48, 663–670.

Dent, J.A., Polson, A.G., Klymkowsky, M.W., 1989. A whole-mount immunocytochemical analysis of the expression of the intermediate filament protein vimentin in *Xenopus*. Development 105, 61–74.

Elinson, R.P., del Pino, E.M., 1985. Cleavage and gastrulation in the egg-brooding, marsupial frog. *Gastrotheca riobambae*. J. Embryol. Exp. Morphol. 90, 223–232.

Elinson, R.P., del Pino, E.M., Townsend, D.S., Cuesta, F.C., Eichhorn, P., 1990. A practical guide to the developmental biology of terrestrial-breeding frogs. Biol. Bull. 179, 163–177.

Ewald, A.J., Peyrot, S.M., Tyszka, J.M., Fraser, S.E., Wallingford, J.B., 2004. Regional requirements for *Dishevelled* signaling during *Xenopus* gastrulation: separable effects on blastopore closure, mesendoderm internalization and archenteron formation. Development 131, 6195–6209.

Faivovich, J., Haddad, C.F.B., Garcia, P.C.A., Frost, D.R., Campbell, J.A., Wheeler, W.C., 2005. Systematic review of the frog family hylidae, with special reference to hylinae: phylogenetic analysis and taxonomic revision. Bull. Am. Mus. Nat. Hist. 294, 1–240.

Gerhart, J., Danilchik, M., Doniach, T., Roberts, S., Rowning, B., Stewart, R., 1989. Cortical rotation of the *Xenopus* egg: consequences for the anteroposterior pattern of embryonic dorsal development. Development (Suppl.) 107, 37–51.

Gont, L.K., Steinbeisser, H., Blumberg, B., De Robertis, E.M., 1993. Tail formation as a continuation of gastrulation: the multiple cell populations of the *Xenopus* tailbud derive from the late blastopore lip. Development 119, 991–1104.

Graham, C.H., Ron, S.R., Santos, J.C., Schneider, C.J., Moritz, C., 2004. Integrating phylogenetics and environmental niche models to explore speciation mechanisms in dendrobatid frogs. Evolution 58, 1781–1793.

Hardin, J., Keller, R., 1988. The behaviour and function of bottle cells during gastrulation of *Xenopus laevis*. Development 103, 211–230.

Harland, R.M., 1991. In situ hybridization: an improved whole-mount method for *Xenopus* embryos. Methods Cell Biol. 36, 685–695.

Hausen, P., Riebesell, M., 1991. The Early Development of *Xenopus laevis*. Springer, Berlin.

Herrmann, B.G., Kispert, A., 1994. The *T* genes in embryogenesis. Trends Genet. 10, 280–286.

Hotta, K., Takahashi, H., Asakura, T., Saitoh, B., Takatori, N., Satou, Y., Satoh, N., 2000. Characterization of *Brachyury*-downstream notochord genes in the *Ciona intestinalis* embryo. Dev. Biol. 224, 69–80.

Kageyama, T., 1980. Cellular basis of epiboly of the enveloping layer in the embryos of the medaka *Oryzias latipes*: I. Cell architecture revealed by silver staining method. Dev. Growth Differ. 22, 659–668.

Keller, R., 1978. Time-lapse cinematographic analysis of superficial cell behavior during and prior to gastrulation in *Xenopus laevis*. J. Morphol. 157, 223–248.

Keller, R., 1986. The cellular basis of amphibian gastrulation. In: Browder, L. (Ed.), Developmental Biology: A comprehensive synthesis: 2. The cellular basis of morphogenesis. Plenum, New York, pp. 241–327.

Keller, R., Shook, D., 2004. Gastrulation in amphibians. In: Stern, C.D. (Ed.),

Gastrulation from Cells to Embryo. Cold Spring Harbor Laboratory Press, New York, pp. 291–304.

Kispert, A., Herrmann, B.G., 1994. Immunohistochemical analysis of the Brachyury protein in wild type and mutant mouse embryos. Dev. Biol. 161, 179–193.

Kuratani, S., Horigome, N., 2000. Developmental morphology of branchiomeric nerves in a cat shark *Scyliorhinus torazame* with special reference to rhombomeres, cephalic mesoderm and distribution patterns of cephalic crest cells. Zoolog. Sci. 17, 893–909.

Lane, M.C., Sheets, M.D., 2006. Heading in a new direction: implications of the revised fate map for understanding *Xenopus laevis* development. Dev. Biol. 296, 12–28.

Nieuwkoop, P.D., Faber, J., 1994. Normal Table of *Xenopus laevis* (Daudin). Garland Publishing, New York.

Santos, J.C., Coloma, L.A., Cannatella, D.C., 2003. Multiple, recurring origins of aposetism and diet specialization in poison frogs. Proc. Nat. Acad. Sci. U. S. A. 100, 12792–12797.

Scharf, S.R., Rowning, B., Wu, M., Gerhart, J.C., 1989. Hyper-dorsoanterior embryos from *Xenopus* eggs treated with D_2O. Dev. Biol. 134, 175–188.

Smith, B.G., 1912. The embryology of *Cryptobranchus allegheniensis*, including comparisons with some other vertebrates: I. Introduction: the history of the egg before cleavage. J. Morphol. 23, 61–157.

Smith, J., 1999. *T*-box genes: what they do and how they do it. Trends Genet. 15, 154–158.

Smith, J.C., Price, B.M.J., Green, J.B.A., Weigel, D., Herrmann, B.G., 1991. Expression of a *Xenopus* homolog of *Brachyury* (*T*) is an immediate-early response to mesoderm induction. Cell 67, 79–87.

Tada, M., Smith, J.C., 2000. *Xwnt11* is a target of *Xenopus Brachyury*: regulation of gastrulation movements via *Dishevelled*, but not through the canonical *Wnt* pathway. Development 127, 2227–2238.

Wacker, S., Grimm, K., Joos, T., Winklbauer, R., 2000. Development and control of tissue separation at gastrulation in *Xenopus*. Dev. Biol. 224, 428–439.

Wallingford, J.B., Fraser, S.E., Harland, R.M., 2002. Convergent extension: the molecular control of polarized cell movement during embryonic development. Dev. Cell 2, 695–706.

Winklbauer, R., Schüferld, M., 1999. Vegetal rotation, a new gastrulation movement involved in the internalization of the mesoderm and endoderm in *Xenopus*. Development 126, 3703–3713.

Winklbauer, R., Medina, A., Swain, R.K., Steinbeisser, H., 2001. *Frizzled-7* signalling controls tissue separation during *Xenopus* gastrulation. Nature 413, 856–860.

Wolpert, L., Jessell, T., Lawrence, P., Meyerowitz, E., Roberson, E., Smith, J., 2007. Principles of Development, Third Edition. Oxford Univ. Press, Oxford, UK.

Youn, W.B., Keller, R.E., Malacinski, G.M., 1980. An atlas of notochord and somite morphogenesis in several anuran and urodelean amphibians. J. Embryol. Exp. Morphol. 59, 223–247.